A Fault Tolerant Superheat Control Strategy for Supermarket Refrigeration Systems

Kasper Vinther[1], Roozbeh Izadi-Zamanabadi[1,2], Henrik Rasmussen[1], and Jakob Stoustrup[1]

***Abstract*— In this paper, a fault tolerant control (FTC) strategy is proposed for evaporator superheat control in supermarket refrigeration systems. Conventional control uses a pressure and temperature sensor for this purpose, however, the pressure sensor can fail to function. A contingency control strategy, based on a maximum slope-seeking control method and only a single temperature sensor, is developed to drive the evaporator outlet temperature to a level that gives a suitable superheat of the refrigerant. The FTC strategy requires no a priori system knowledge or additional hardware and functions in a plug&play fashion. The strategy is outlined by means of procedural steps as well as a flow chart that also illustrates the process of automatic tuning of the maximum slope-seeking controller. Test results are furthermore presented for a display case in a full scale CO_2 supermarket refrigeration system.**

I. Introduction

Maintaining temperature of the foods within predefined intervals has the highest priority in the refrigeration systems of supermarkets/stores as it has direct impact on quality and safety requirements. In addition, enrolling maintenance people, when a fault occurs in the system, will increase the operation costs substantially. These are some of the natural incentives for the attempts to develop fault-tolerant control (FTC) strategies. In supermarkets, goods are stored in display cases/freezers until they have been purchased by the customers. Fig. 1 conceptually illustrates the basic functionality of such units: The inlet air traverse over the evaporator, by means of fans, and exchanges heat with the refrigerant that flows inside the evaporator. The resulting cold air maintains the cold air curtain and hence the goods temperature at a desired level. The cooling process in each of these refrigeration units is regulated by means of controlling the mass flow of the refrigerant in the corresponding evaporator unit using an electronic expansion valve (EEV). The objective of controlling the mass flow into the evaporator is to fill the evaporator and thereby maximize the heat transfer between the air and the refrigerant inside the evaporator. At the same time, flooding the evaporator, such that there exists refrigerant in liquid state at the outlet of the evaporator, should be avoided as it could harm the compressors. To be able to measure the distance of the liquid/gas boundary from the outlet of the evaporator, two sensors are predominantly used: a temperature sensor which measures the refrigerant temperature at gas state at the outlet of evaporator and a pressure sensor that provides the evaporation pressure (and hence evaporation temperature). The difference between these two temperatures is called superheat and can be used as an indication for how far the liquid/gas boundary is from the outlet. Ideally, the superheat (SH) should be small (positive). A $SH = 0$ indicates that the evaporator is flooded.

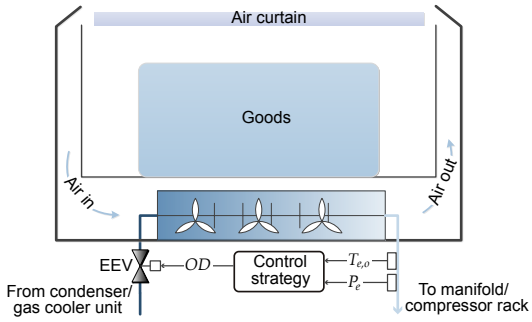

Fig. 1. Conceptual illustration of a refrigeration unit (display case / freezer).

Loosing the ability of appropriately controlling the mass flow will have: a) dire consequences on the quality of goods in the corresponding refrigeration unit, and b) possibility for degrading the compressor unit's performance. Therefore, there is a need for a control strategy that can be activated as a contingency control option when a sensor fault occurs. The areas of fault diagnosis and fault-tolerant control has been subject to intense research in the past three decades resulting in a large amount of well-developed and well-documented theoretical methods and approaches ([1], [2], [3], [4]). In [5] we initially proposed an evaporator unit of a residential air condition (RAC) as a benchmark for FTC. This paper provides an innovative FTC solution that will be utilized as contingency control for refrigeration units in supermarkets/stores so that the control functionality is preserved even in the case of a (pressure) sensor failure. Our approach is based on maximum slope-seeking (MSS) control, where the basic idea is to utilize the inherent nonlinear characteristics of the outlet temperature behavior at the vicinity of the evaporation temperature, which can be detected by actively perturbing the system dynamics. This is done instead of trying to estimate the evaporation temperature in a reliable and robust manner, which is a difficult task and requires full system knowledge. Estimating the temperature is also challenging since each system is different, subject to changing operating conditions, and nonlinear.

MSS was first presented by the authors in [6] and applied with success to different refrigeration systems in [7] and [8]. Stability was later studied in [9]. In this paper

[1]K. Vinther, H. Rasmussen, R. Izadi-Zamanabadi, and J. Stoustrup are with the Section of Automation and Control, Department of Electronic Systems, Aalborg University, 9220, Denmark {kv,hr,riz,jakob}@es.aau.dk

[2]R. Izadi-Zamanabadi is with the Department of Electronic Control and Services, Danfoss A/S, 6430, Denmark roozbeh@danfoss.com

we will investigate automatic tuning of the controller due to the fact that evaporators and refrigeration systems in supermarkets are of different shape and sizes and hence differ in their dynamics. Therefore, the developed controller has to function in a plug&play [10] fashion by identifying the underlying system dynamics and determining its own parameters. Further requirements that must be fulfilled are: flooding avoidance, maintaining low superheat, and being robust against changes in operating conditions (such as suction pressure, load, and ambient temperature).

The paper is organized as follows: A short description of supermarket refrigeration systems is provided in Section II and the problem associated with sensor fault is explained. Section III provide a short introduction to the MSS control method. Section IV provides strategies for immediate reaction to a flooding situation. In Section V we describe the procedure that is used to automatically tune the controller. Test results of the developed method on a display case in a full-scale supermarket system is finally presented.

II. CO2 Supermarket Refrigeration System

Supermarket refrigeration systems typically have a physical configuration as shown in Fig. 2. The refrigerating units are divided in two zones - a low temp. zone and a medium temp. zone. Low temp. zones typically include the freezers and the medium temp. zones include refrigerators. Furthermore, dedicated compressor racks are employed to maintain an appropriate suction pressure in each zone. The display cases/freezers in each zone operate either individually or in an "island" configuration, i.e. a group of refrigeration units that share some sensors like a pressure sensor.

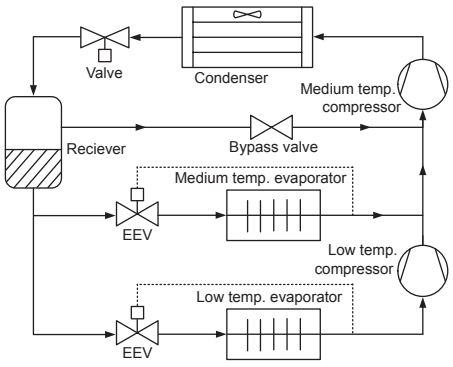

Fig. 2. Typical configuration of a medium-sized supermarket refrigeration system. Only one medium and one low temperature evaporator is shown out of many in parallel (each having its own valve and superheat control).

A. The Control Challenges

Measurements from pressure sensors are instrumental for calculating the superheat defined as:

$$SH = T_{e,o} - T_e \tag{1}$$

where $T_{e,o}$ is the temperature of the refrigerant in gas form measured at the outlet of the evaporator and $T_e = f_e(P_e)$ is the evaporation temperature obtained with the measured evaporation pressure P_e. f_e is an injective function and is commonly realized by means of dedicated thermodynamic tables. The common approach to superheat control is to compare the calculated SH (based on the $T_{e,o}$ and P_e measurements) with a predefined SH_{ref} and manipulate the opening degree (OD) of the related EEV by means of a dedicated control strategy (PI(D) controllers are commonly used). When the pressure sensor measurements become faulty then the calculated SH will become erroneous and, hence, the control algorithm will fail to function.

B. Pressure Sensor Failure

The evaporation pressure sensor may fail to operate due to a combination of oil and impurities/dirt blocking a passage in the device. When the fault occurs the measurement signal "freezes". This phenomenon can be described as:

$$P_{e,m}(t) \equiv P_{e,0} \qquad \text{for } t \geq t_0$$

where $P_{e,0}$ is the last healthy measurement signal at time t_0.

C. Detection Procedure

As mentioned the faulty sensor will deliver a constant signal. The only variations in the measurements will be due to the digitizing accuracy in the A/D converters. In this case the following hypothesis can be established:

$$\begin{aligned} \mathcal{H}_0 &: \sigma^2(t) > \sigma_0^2 \qquad \text{no fault,} \\ \mathcal{H}_1 &: \sigma^2(t) \leq \sigma_0^2 \qquad \text{fault,} \end{aligned}$$

where $\sigma^2(t)$ is the variance of the test signal and σ_0^2 is defined based on the used A/D converters digitalization precision. The test signal is obtained by first high pass filtering the signal and then using a statistical detection method such as CUSUM to identify the relevant hypothesis.

III. Maximum Slope-seeking Control

The purpose of MSS control is to drive a nonlinear system towards a maximum in the slope of the system's steady state I/O-map. The method is therefore applicable if such an extremum is also a desired/optimal operating point. A requirement is that the maximum slope point is unique in the operating range, which is ensured if the static nonlinearity is smooth and has a bell shaped first derivative, which is either non-positive or non-negative. Functions having these properties are called sigmoid functions.

The MSS method relies on perturbation of the system and is closely related to the more general slope-seeking control presented in e.g. [11]. Fig. 3 illustrates the structure of MSS control. It is assumed that the system to be controlled

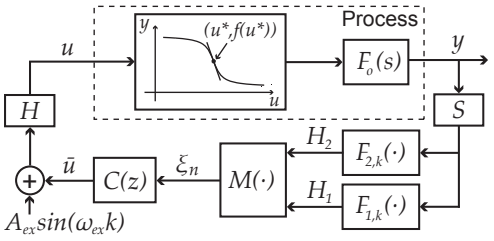

Fig. 3. Structure of MSS control applied to a nonlinear system.

can be adequately approximated by a Hammerstein model structure with a static nonlinearity $f(u)$ with sigmoid function properties and linear output dynamics F_o. The desired operating point is denoted $(u^*, f(u^*))$ and the objective is to drive the input offset $\bar{u}$ towards the unknown optimal input u^*. This is achieved by perturbing the system with a sine signal $A_{ex}\sin(\omega_{ex}k)$ and sampling the output y. The sampled signal is then filtered with periodic FIR filters $F_{1,k}$ and $F_{2,k}$, with k being the discrete time index. These filters are periodic with period $T_{ex} = \frac{2\pi}{\omega_{ex}}$ and they extract the first and second harmonic (H_1 and H_2) of the perturbation signal in the output y. The second harmonic (and higher harmonics) is generated by the curvature of the I/O-map. If we assume that the I/O-map is symmetric around the maximum slope point, then the mean curvature experienced by the perturbation will be zero in this point and positive and negative to each side, respectively, which can then be used for feedback purposes. The convergence will be offset if the function is not symmetric around the maximum slope point, however, if the perturbation amplitude is chosen sufficiently small, then this potential offset will become negligible. The real part of the complex second harmonic could in principle be used as a feedback signal alone. However, if the phase shift caused by dynamics in the system is larger than 90 degrees, then the sign of the feedback signal should be changed. The cross product defined in $\mathbb{R}^2$ between the first and second harmonic is therefore taken so that we will only have to ensure that the difference in phase shift between these two frequencies is less than 90 degrees, which is easier to ensure, since they are only an octave apart. Furthermore, a normalization of the resulting error signal, with respect to the first harmonic, is performed giving ξ_n. This signal is then integrated in C and with proper choice of integral gain then $\bar{u} \to u^*$ as $k \to \infty$. The periodic FIR filters, the normalized cross product, and the integral control are defined as

$$F_{p,k}(y) = \frac{2}{N}\sum_{n=1}^{N} y(k-N+n)$$
$$(\cos(p\omega_{ex}(n+k-\phi)) - j\sin(p\omega_{ex}(n+k-\phi))), \quad (2)$$
$$M(H_1,H_2) = \frac{|H_1||H_2|\sin(\theta_{12})}{|H_1|^2} = \frac{|H_2|\sin(\theta_{12})}{|H_1|}, \quad (3)$$
$$C(z) = \frac{Kt_s}{z-1}, \quad (4)$$

where $p = [1, 2]$ is the harmonic, N is the number of samples in one period T_{ex}, θ_{12} is the angle from the first harmonic to the second, K is the integral gain, and t_s is the sample time. ϕ is an optional phase shift compensation, which is useful if the delay in the system is large. Anti-windup in the integral control is necessary if the input u has saturation limits and the integral control should not be activated before a full period of N samples of y is available after startup.

As a general guideline, the control should be tuned so that the system dynamics is faster than the periodic perturbation, which at the same time should be faster than the integral control. More detail on the MSS control method and tuning of it can be found in our previous work [6], [7], [8], [9]. In this paper we will tune the control by acquiring an approximate Hammerstein model of the system, which can be used to find appropriate control parameters through simulation. The procedure is explained in Section V, however, before that a simulation example is given using parameters identified from the supermarket refrigeration system described in Section II.

Fig. 4 shows the simulation result using (5) and (10) as system model, with the system and control parameters given in Table I. The input u to the system is the valve opening

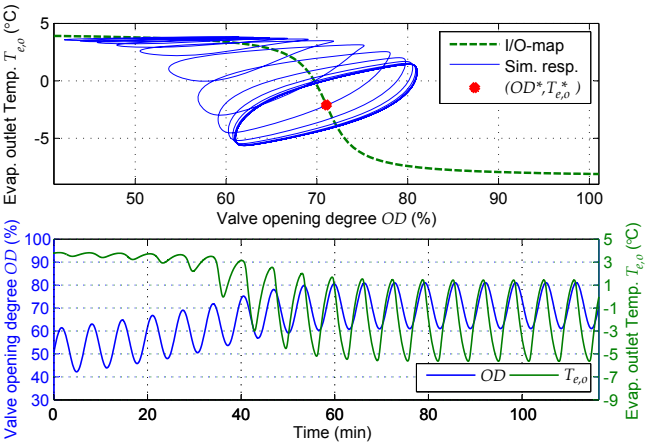

Fig. 4. Simulation example showing convergence using maximum slope-seeking. The top graph shows the steady state I/O-map, the simulation response, and the maximum slope point $(OD^*, T^*_{e,o})$. The bottom graph shows the time evolution of the input and output in the same simulation.

degree OD in percentage, the output y is the evaporator outlet temperature $T_{e,o}$ and the input is perturbed with a sinusoidal signal. The offset OD (corresponding to $\bar{u}$ in Fig. 3) starts 20% away from OD^* and has converged after about 55 min. The top graph in Fig. 4 also shows how the output ends up circling around the desired operating point $(OD^*, T^*_{e,o})$ due to the continouos input perturbation and the system dynamics. Note that the MSS controller does not use the system model and does not know where the desired operating point (maximum slope point) lies, but does converge to this point, which gives a superheat that corresponds to a close to optimal filling of the evaporator. This means that the evaporator filling can be controlled by only measuring the outlet temperature $T_{e,o}$ in cases where the pressure sensor measurement is faulty.

IV. Safety Logic

The proposed MSS is a relatively slow adaptive control method. Safety logic is therefore added in the evaporator filling control case, since it is important to react fast if large changes in compressor speed or load suddenly occurs. These changes can quickly flood the evaporator, which should be avoided. The compressor speed is assumed unknown. However, the amplitude of the first harmonic of the perturbation signal measured at the output gets small when the evaporator floods and if it has a very low filling, see e.g. Fig. 4.

The safety logic switches to a recovery mode if the amplitude of the first harmonic is consistently small. A step

back in OD is made, when entering recovery mode, to ensure that the evaporator is not flooded. A check is then made to see if the low amplitude was caused by a low flow situation or a flooding situation. This is detectable by looking at $T_{e,o}$, which will only have a large change after a step back in OD from the flooding situation. The input offset $\bar{u}$ (in this case $\bar{OD}$) is then slowly ramped up until the amplitude of the first harmonic is above an upper threshold. If it was a low flow situation, the ramping can start from the original OD before a step back was made. The safety logic is described in more detail in [8] and also shown in Fig. 5.

V. Autotuning Procedure

A procedure is proposed in the following for automatic tuning of the MSS control. The control parameters, which have to fit the particular system, are the perturbation period T_{ex}, which should be chosen relative to the system time constant, the phase shift compensation ϕ, which can be set to match the system delay, and finally the integral gain K, which has to match the nonlinearity of the system. The perturbation amplitude A_{ex} is not highly critical. Multiple tests have shown that a fixed value of $A_{ex} = 10$ gives an adequate perturbation on different refrigeration systems compared to the noise level and disturbances.

An model giving the relationship between the input OD and the output $T_{e,o}$ is derived to be able to choose a suitable integral gain K through simulation. A good approximation of the static nonlinear I/O-map is given as

$$T_{e,o} = -k_1 atan\left(k_2\left(OD + OD^*\right)\right) + T^*_{e,o}, \tag{5}$$

where k_1, k_2, $T^*_{e,o}$, and OD^* should be fitted so that the model matches the real system. This approximation have shown to fit well with measurements (see e.g. [8]) and (5) has sigmoid function properties with horizontal asymptotes determined by the evaporation temperature (lower bound) and the temperature of the air flowing across the evaporator (upper bound). A slow ramping of the input reveals the static I/O-map and the parameters are fitted in the following way:

$$k_1 = \frac{\left(T_{e,o,max} - T_{e,o,min}\right)}{\pi}, \tag{6}$$

where $T_{e,o,max}$ and $T_{e,o,min}$ are the maximum and minimum temperature, respectively, encountered during the slow ramp test going from a low OD to a high OD. The offset temperature $T^*_{e,o}$ is calculated as

$$T^*_{e,o} = \frac{\left(T_{e,o,max} + T_{e,o,min}\right)}{2}, \tag{7}$$

and the offset opening degree OD^* corresponding to $T^*_{e,o}$ is determined by going through the measured data during the ramp test. These two values are also a good estimate of the real maximum slope point in the system. Finally, a range of k_2 values is simulated and the one with best match to the test data is used. Using the 1-norm (instead of 2-norm) as error measure between model and data gives a good indication of fitness in cases with a lot of disturbances.

The ramp test needs to be stopped before the evaporator is fully flooded. This can be achieved by calculating the rate of change of a filtered version of the outlet temperature $T_{e,o}$ denoted RoC. The maximum slope point is passed when a clear negative peak in RoC is detected, which means that the test can be stopped. The equations involved are;

$$T_{e,o,f}(k) = T_{e,o,f}(k-1)\frac{\tau - t_s}{\tau} + T_{e,o}(k)\frac{t_s}{\tau}, \tag{8}$$

$$RoC(k) = \frac{T_{e,o,f}(k) - T_{e,o,f}(k-1)}{t_s}, \tag{9}$$

where $T_{e,o,f}$ is the filtered $T_{e,o}$ with filter coefficient τ and sample time t_s. $T_{e,o}$ also needs to drop at least 4-5 K from the starting value at low OD, in order to remove false detections of a peak in RoC and a maximum time horizon from the last detected peak is used to know when to stop searching for the peak. Note that the RoC is also used as a quick evaporator refill algorithm during control of the display case air temperature T_{air}, which is controlled using conventional valve on/off hysteresis temperature control. The evaporator is emptied for refrigerant due to the valve off period and when T_{air} reaches the upper temperature threshold, where the valve switches on again, the refill algorithm will run first with high OD to quickly fill the evaporator and to maximize the heat transfer. When the RoC peak is detected the normal PI(D) or MSS control takes over and ensures a suitable superheat level in the valve on period.

The dynamics of the system are also approximated. As suggested in [5], a simple FOPDT model is used and identified using the biased relay feedback method, see e.g. [12], [13]. The FOPDT model is given as

$$F_o(s) = \frac{1}{\left(T_{sys}s + 1\right)}e^{-sT_d}, \tag{10}$$

where T_{sys} is the system time constant and T_d is the delay. The delay can be determined as the time from a step in the input is made to a change in the output is observed, and it is detectable in the transition from the ramp test to the relay feedback test, where we start by stepping OD down. Three relays are made before the ultimate gain K_u and period T_u is determined. These values can be used to determine the system time constant and K_u is given as

$$K_u = \frac{4A_i}{\pi A_o}, \tag{11}$$

where A_i is the input amplitude of the relay and A_o is the output amplitude. T_u is the total time of one relay (one low plus one high OD period). The time constant is then

$$T_{sys} = \frac{2\pi\sqrt{\left(K_u K_{sys}\right)^2 - 1}}{T_u}, \tag{12}$$

$$K_{sys} = \frac{\int^{T_u}\left(T_{e,o}(t) - T_{e,o,ref}(t)\right)dt}{\int^{T_u}\left(OD(t) - OD_{offset}(t)\right)dt}, \tag{13}$$

where $T_{e,o,ref} = T^*_{e,o}$ and OD_{offset} is OD value where the relay is centered around. The gain K_{sys} accounts for the nonlinearity and K_{sys} is therefore set to 1 in (10) when both the static nonlinear model and dynamic model are used.

The system dynamics should be faster than the perturbation and the identified system specific T_{sys} can therefore be

used to determine a suitable T_{ex}. The perturbation should at the same time not be too slow, however, to also account for parameter uncertainty T_{ex} is set to four times T_{sys}.

The final parameter K can now be determined based on the identified models given in (5) and (10). Here we make a convergence test, where the system is started away from the desired operating point and K is then iterated using the bisect algorithm to a value which gives exactly 5% overshoot. K is finally divided by two to account for model uncertainty. A flowchart of the code implementation is shown in Fig. 5.

VI. Test Results

The automatic tuning procedure and MSS control is tested by inducing a pressure sensor fault in software. Nominal PI control of the superheat with on/off temperature control on the display case air temperature T_{air} is first carried out and after 30 min the fault is induced. This starts the automatic tuning procedure and the test result is shown in Fig. 6.

The ramp test is performed after the pressure sensor fault. A zoomed graph shows $T_{e,o}$ and the fitted static nonlinear model. The data does not show a smooth S-shaped curve due to disturbances in the evaporation pressure, but the model does show a good fit. The ramp test also stops before the evaporator gets fully flooded as expected and the relay feedback test takes over. The identified parameters are presented in Table I. The MSS control then takes over

TABLE I

Identified system model and autotuned control parameters.

	Parameter	Value
Static model	k_1 (-)	4.02
Static model	k_2 (-)	0.44
Static model	$T^*_{e,o}$ ($^\circ C$)	-2.10
Static model	OD^* (%)	71.04
FOPDT model	T_{sys} (s)	96.95
FOPDT model	K_{sys} (-)	-0.40
FOPDT model	T_d (s)	87
Ctrl. par.	ϕ (s)	87
Ctrl. par.	T_{ex} (s)	388
Ctrl. par.	A_{ex} (-)	10
Ctrl. par.	K (-)	0.0285

approximately 71 min into the test (41 min after sensor fault). The display case air temperature T_{air} is not controlled during the automatic tuning procedure and therefore reaches approximately -3 degree. However, the surface temperature of the goods in the display case T_{surf} stays between 0-5 degree. The valve on time is only 4-5 min before T_{air} reaches the lower limit, due to a relatively aggressive evaporator and refrigerant. This means that only the refill evaporator algorithm runs and the MSS control does not have time to run. The T_{air} control is therefore deactivated 125 min into the test to see how the MSS controller performs. The last part of the test shows how the MSS controller adapts the average OD from 71% to roughly 50% giving a better $T_{e,o}$ and more appropriate filling of the evaporator. The superheat during the test is shown in Fig. 7. The nominal control first brings the superheat to the typical reference at 12 K and the T_{air} temperature control then kicks in giving an average

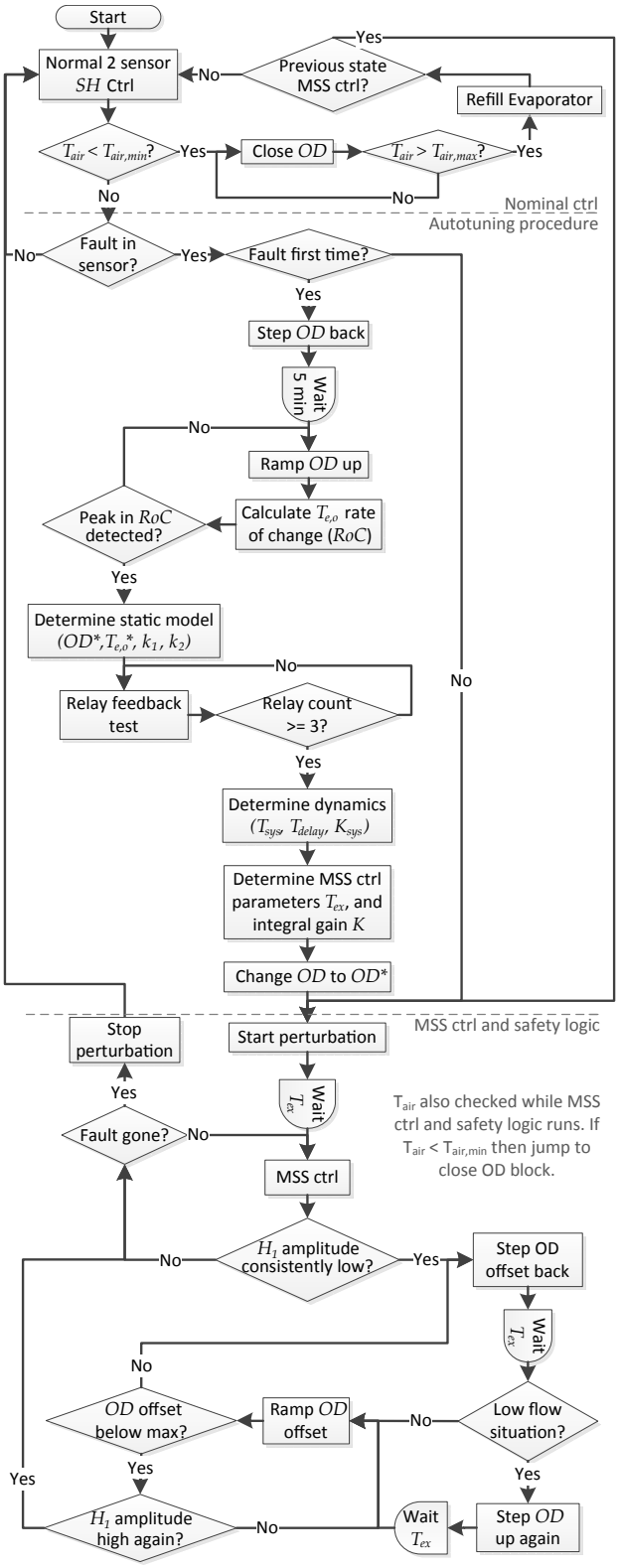

Fig. 5. Flowchart overview of code implementation.

superheat of approximately 18 K during the first 30 min of the test. The same average superheat is also obtained with MSS with T_{air} control (71 to 125 min into test). An average superheat of 6 K can be maintained with MSS without T_{air}

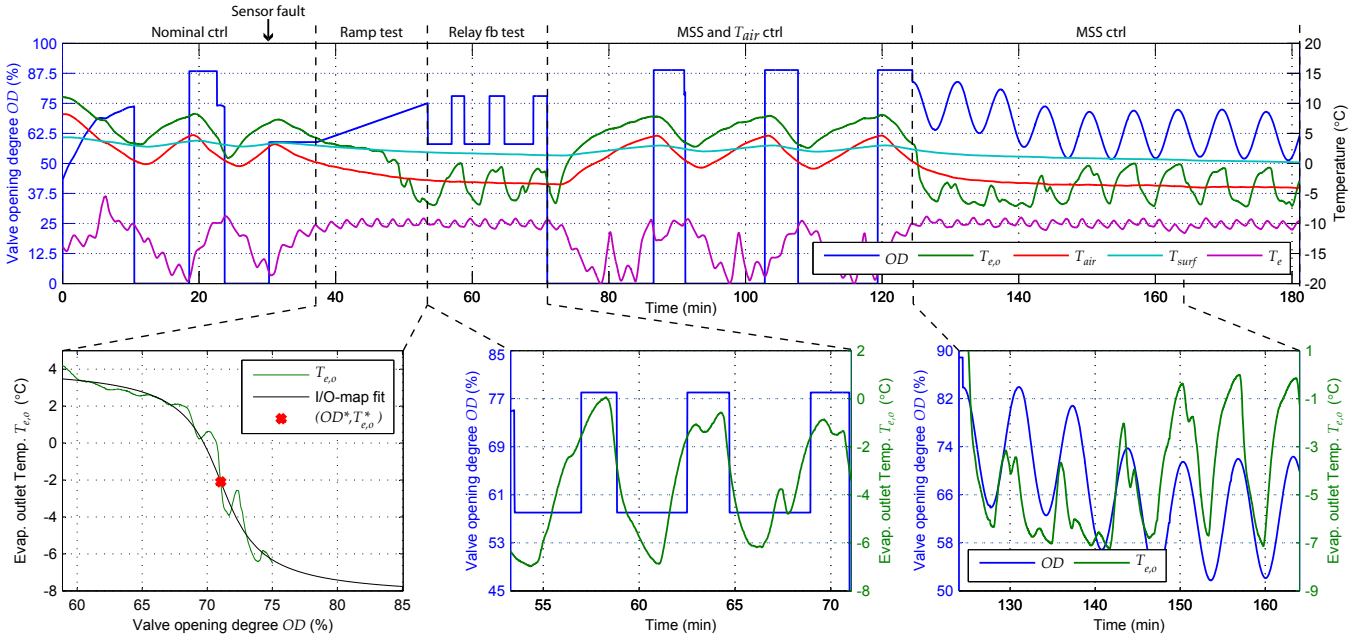

Fig. 6. Result from 3 hour test. Only $T_{e,o}$ and T_{air} are used in the code, however, T_e and T_{surf} are shown as well for comparison.

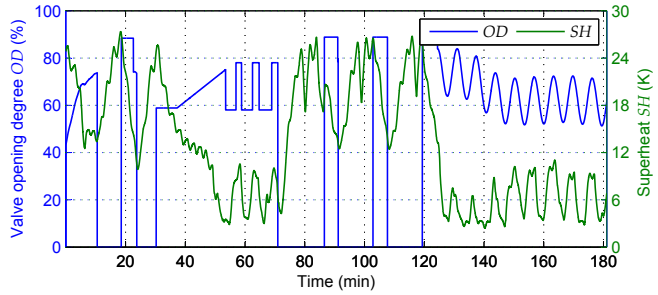

Fig. 7. Valve OD and superheat SH during 3 hour test.

control, which gives a high efficiency of the evaporator.

The superheat control challenge and performance benchmark outlined in [5] is mostly valid for a one compressor one evaporator systems. However, the proposed contingency control have shown to fulfill the outlined objectives. Potential improvements could involve having more relays and thus taking an average of the identified parameters if there are a lot of disturbances in the system. However, only an approximate model is needed for tuning purposes.

VII. Conclusion

Pressure sensors are expensive and in refrigeration systems they sometimes experience freezing or could break. This can give problems because the evaporator filling or superheat level is conventionally controlled with this sensor and a temperature sensor placed at the outlet of the evaporator. We have shown how a novel MSS controller can be used as an FTC method, when a pressure sensor fault occurs, which can prevent deterioration of the foodstuff in the display cases. An automatic tuning procedure is proposed and tests have shown the effectiveness of the MSS method in keeping a low superheat and thus a high efficiency. The method does not require additional hardware or a priori system knowledge and also has potential as a cheap one sensor alternative to the conventional two sensor solution. Future work include tests on other refrigeration systems for longer periods of time.

References

[1] J. Chen and R. J. Patton, *Robust Model-Based Fault Diagnosis for Dynamic Systems*. Springer, 1998.

[2] J. J. Gertler, *Fault Detection and Diagnosis in Engineering Systems*, 1st ed. Marcel Dekker Inc., 1998.

[3] M. Blanke, M. Kinnaert, J. Lunze, and M. Staroswiecki, *Diagnosis and Fault-Tolerant Control*. Springer, November 2010.

[4] R. Isermann, *Fault-Diagnosis Systems, An introduction from fault detection and fault tolerance*. Springer, 2006.

[5] R. Izadi-Zamanabadi, K. Vinther, H. Mojallali, H. Rasmussen, and J. Stoustrup, "Evaporator unit as a benchmark for Plug and Play and fault tolerant control," in *8th IFAC Symposium on Fault Detection, Supervision and Safety of Technical Processes*, Mexico City, Mexico, 2012, pp. 701–706.

[6] K. Vinther, H. Rasmussen, R. Izadi-Zamanabadi, and J. Stoustrup, "Utilization of Excitation Signal Harmonics for Control of Nonlinear Systems," in *IEEE International Conference on Control Applications*, Dubrovnik, Croatia, 2012, pp. 1627–1632.

[7] ——, "Single Temperature Sensor based Evaporator Filling Control using Excitation Signal Harmonics," in *IEEE International Conference on Control Applications*, Dubrovnik, Croatia, 2012, pp. 757–763.

[8] ——, "Single temperature sensor superheat control using a novel maximum slope-seeking method," *International Journal of Refrigeration*, vol. 36, no. 3, pp. 1118–1129, 2013.

[9] ——, "Maximum Slope-seeking Control of Nonlinear Systems Using Excitation signal Harmonics," 2013, . Submitted for publication.

[10] J. Stoustrup, "Plug & play control: Control technology towards new challenges," *European Journal of Control*, vol. 15, no. 3-4, pp. 311–330, May-August 2009.

[11] K. B. Ariyur and M. Krstic, *Real-Time Optimization by Extremum-Seeking Control*. Wiley-Interscience, 2003.

[12] S.-H. Shen, J.-S. Wu, and C.-C. Yu, "Use of Biased-Relay Feedback for System Identification," *AIChE Journal*, vol. 42, no. 4, pp. 1174–1180, 1996.

[13] Q.-G. Wang, C.-C. Hang, and B. Zou, "Low-Order Modeling from Relay Feedback," *Ind. Eng. Chem. Res.*, vol. 36, no. 2, pp. 375–381, 1997.